Comparison of Solution Structural Flexibility and Zinc Binding Domains for Insulin, Proinsulin, and Miniproinsulin†

Niels C. Kaarsholm,‡ Hui-Chong Ko,§ and Michael F. Dunn*,§

Department of Biochemistry, University of California at Riverside, Riverside, California 92521, and Novo Research Institute, DK-2880 Bagsvaerd, Denmark

Received July 18, 1988; Revised Manuscript Received December 14, 1988

ABSTRACT: The chromophoric divalent metal ion chelators 4-(2-pyridylazo)resorcinol (PAR) and 2,2′,2″-terpyridine (terpy) are used as kinetic and spectroscopic probes to investigate in solution the SCN^--induced conformational transformations of the insulin, proinsulin, and miniproinsulin hexamers (miniproinsulin is a proinsulin analogue wherein the C-chain is replaced by a dipeptide cross-link between Gly-A1 and Ala-B30). Herein we designate the 2Zn and 4Zn crystal forms of the hexamer as the T_6 and T_3R_3 conformations, respectively. For all three proteins, addition of SCN^- reduces the rate of sequestering and removal of zinc ion by chelator. The effect of SCN^- on the rate of this process saturates at the same concentration (30 mM) known to induce the T_6 to T_3R_3 transformation in the insulin crystal. Under both T_6 and T_3R_3 conditions, the critical stoichiometry for high-affinity interaction between Zn^{2+} and each of the three proteins is shown to be 2 mol of Zn^{2+}/mol of protein hexamer. Consequently, we confirm the finding that off-axial coordination of Zn^{2+} via His-B10 and His-B5 residues is of minor importance for the SCN^--induced conformation change in solution [Renscheidt, H., Strassburger, W., Glatter, U., Wollmer, A., Dodson, G. G., & Mercola, D. A. (1984) *Eur. J. Biochem. 142*, 7–14]. Under T_6 conditions, the kinetics of the reactions between insulin, proinsulin, and miniproinsulin and a variable excess of terpy are similar and biphasic. The fast phase of each reaction is first order in terpy and first order in protein-bound Zn^{2+} ($k = 0.5–1.4 \times 10^4$ M^{-1} s^{-1}) and involves the formation of a terpy–Zn^{2+}–protein complex at each zinc site. The slow phase of each reaction is first order in terpy at low concentrations and tends toward a limiting, saturated value at high [terpy]. In each system, this step involves the rate-limiting dissociation of terpy-bound Zn^{2+} from the protein, followed by the rapid coordination of a second terpy molecule and formation of $(terpy)_2Zn^{2+}$. Under T_3R_3 conditions, the corresponding reactions for the three proteins are also very similar and biphasic. When compared to T_6 conditions, the second-order rate constant of the fast phase is slightly reduced ($k = 0.5–0.6 \times 10^4$ M^{-1} s^{-1}). The rate of the slow phase is remarkably reduced ($k = 0.005$ s^{-1}) and becomes zeroth order in terpy. The striking similarity between the kinetic parameters shows that the same process is rate-limiting for the reaction of terpy with the SCN^--induced form of each protein. The kinetic results indicate a mechanism where one of two zinc environments per hexamer is transformed by SCN^-. We conclude that the slow rate observed under T_3R_3 conditions likely is limited by the rate of the SCN^--induced conformational change. Studies of the rate of removal of Zn^{2+} from the insulin hexamer under conditions similar to those which give an R_6 crystal form provide further evidence consistent with these conclusions.

In mammals, insulin is synthesized in the β-cells of the pancreas. Synthesis involves a complex and incompletely understood sequence of posttranslational events that include the conversion of preproinsulin to proinsulin, the packaging of proinsulin in secretory granules, the assembly of proinsulin hexamers, the conversion of proinsulin hexamers to insulin hexamers, and the formation of crystalline arrays of hexamers in mature granules (Howell et al., 1969; Steiner, 1976; Permutt, 1981). The high concentrations of Zn^{2+} and Ca^{2+} found in these granules (Howell, 1974; Havu et al., 1977) indicate a functional role of both ions during the later stages of biosynthesis.

The X-ray diffraction studies of hexameric insulin provide refined, high-resolution structures of two rhombohedral crystal forms and a monoclinic form known as the 2Zn,[1] 4Zn, and phenol-induced insulin species, respectively (Schlichtkrull, 1958; Blundell et al., 1972; Peking Insulin Structure Research Group, 1974; Bentley et al., 1976; Dodson et al., 1979; Sakabe et al., 1981; Smith et al., 1984; Baker et al., 1988; U. Derewenda, Z. Derewenda, E. Dodson, G. Dodson, C. Reynolds, and D. Smith, private communication). All three forms are torus-shaped molecules. The subunits are arranged as three equivalent dimers associated about the 3-fold axis to form a hexamer. Asymmetry in the dimer produces two different subunit conformations in the hexamer. In the 2Zn and phenol-induced structures, the conformational differences that give rise to asymmetry are small. In the 4Zn structure, the conformational differences are large; one subunit retains a conformation almost identical with that found in 2Zn insulin, while the other subunit has a large change in the conformation

† Supported by the Southern California Affiliate of the American Diabetes Association, NIH Grant PHS-1-RO1-AM31138, the Novo Research Institute, and a grant-in-aid to N.C.K. from the Danish Natural Science Research Council.

* Address correspondence to this author.

‡ Novo Research Institute.

§ University of California at Riverside.

[1] Abbreviations: In, insulin monomer; $(In)_6(Zn^{2+})_2$, 2Zn insulin, or T_6, the crystalline two-zinc hexamer; 4Zn insulin or T_3R_3, the crystalline hexamer species formed in the presence of SCN^- or other members of the lyotropic anion series (Cl^-, Br^-, or I^-); R_6, the crystalline hexamer species formed in the presence of phenol; miniproinsulin, the proinsulin homologue in which the length of the connecting C-peptide is reduced to a dipeptide; P, protein; che, chelator; terpy, 2,2′,2″-terpyridine; PAR, 4-(2-pyridylazo)resorcinol; Tris, 2-amino-2-(hydroxymethyl)-1,3-propanediol.

0006-2960/89/0428-4427$01.50/0

Chart I: Principal Differences between the Crystalline 2Zn (T_6) and 4Zn (T_3R_3) Forms of the Insulin Hexamer[a]

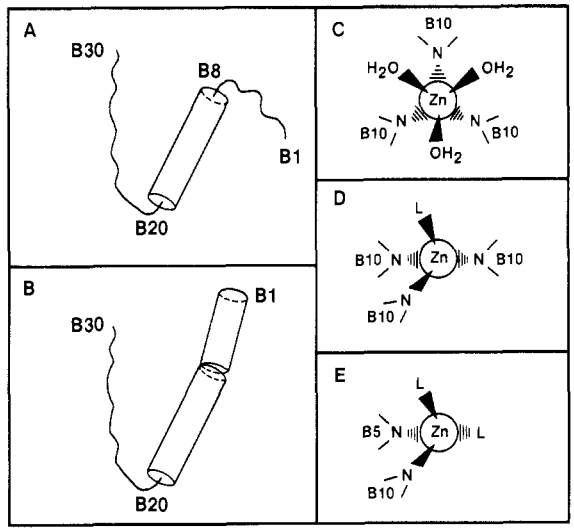

[a] In T_6 insulin, the B-chain of each subunit has α-helix between residues B9 and B19 (panel A). In three of the six subunits in T_3R_3 insulin, the B-chain α-helix extends through residues B1–B19 (panel B). The two axial Zn^{2+} in T_6 insulin and one axial Zn^{2+} in T_3R_3 insulin reside in octahedral ligand fields (panel C). In the transformed B-chain (panel B), two orientations of His-B10 form two types of (partially occupied) tetrahedral zinc sites buried in the T_3R_3 hexamer. One orientation results in an axial His-B10 site (panel D), while the other creates three off-axial His-B10, His-B5 sites (panel E). However, the total Zn^{2+} occupancy reported for T_3R_3 is 2.67 (Smith et al., 1984). L represents H_2O or a lyotropic anion.

of the B-chain. In 2Zn hexamers, the conformation of all six B-chains consists of two sections of extended polypeptide chain connected by a central segment of α-helix, B9-B19. The 2Zn to 4Zn transition results in the conversion of residues B1–B8 from an extended conformation to α-helix in three of the six subunits (structures A and B of Chart I). This causes B1 to move 20–25 Å. In the phenol-induced structure, all six of the insulin subunits have the B1 to B19 helical structure. The 2Zn to 4Zn crystal transformation can be elicited by soaking the crystalline 2Zn hexamer in high concentrations of anions without disturbing the crystal lattice. Alternatively, the 4Zn form can be crystallized directly. The effectiveness of anions that stabilize the 4Zn form follows the Hoffmeister lyotropic series (De Graaff et al., 1981). The monoclinic, phenol-induced form is crystallized in the presence of phenol (De Graaf et al., 1981; Harding et al., 1966).

The two His(B10) metal binding sites of the 2Zn structure are separated by 15.9 Å and located on the 3-fold symmetry axis in the central solvent-filled cavity that runs through the hexamer. Each zinc ion is coordinated in a distorted octahedral ligand field consisting of three His-B10 imidazolyl groups and three water molecules (structure C, Chart I). The coordination geometry in the 4Zn structure is more complex. At one face of the hexamer, a single octahedral Zn^{2+} site is formed on the 3-fold axis from the three symmetry-related His-B10 residues and three water molecules as in the 2Zn form (viz., structure C). At the other face of the hexamer, the helical conformation of the B1–B8 segments of the other three B-chains brings the His-B5 and His-B10 rings from adjacent subunits close together, creating two types of additional (putative) zinc sites (structures D and E). At these faces, the His-B10 side chain exists in two distinct orientations. One orientation (structure D) results in the formation of a zinc site with tetrahedral geometry on the 3-fold axis. The three symmetry-related His-B10 side chains and a chloride ion (or water molecule) are the ligands at this site. Rotation of each HisB10 side chain about the α–β C–C bond to the new orientation brings each imidazole ring into close proximity with the imidazole ring of His-B5 from the neighboring subunit. This orientation creates a total of three identical zinc sites located off the 3-fold axis. These sites involve four ligands in a tetrahedral ligand field [two chloride ions (or water molecules) and two histidyls, His-B5 and His-B10, structure E]. However, the most recent crystal structure results show that the tetrahedral sites are not fully occupied (Smith et al., 1984).

The phenol-induced hexamer contains 2 mol of Zn^{2+}/hexamer and six phenol molecules bound to six essentially identical sites. Each zinc site lies on the symmetry axis and is formed by three His-B10 imidazolyl ligands and a water molecule arranged in a distorted tetrahedral ligand field. The phenol molecules are located in essentially identical hydrophobic pockets. Each pocket is bound on one side by the B-chain helix and on the other three sides by the A-chain. This arrangement places phenol in the off-axial metal sites identified in the 4Zn structure and apparently prevents zinc from binding to these loci.

Since the species designated the 2Zn hexamer is capable of binding more than two zinc ions (Emdin et al., 1980), while in the crystal the species designated the 4Zn insulin hexamer does not bind four zinc ions (an occupancy of 2.67 is reported; Smith et al., 1984), we introduce a new nomenclature to describe the different crystallographically characterized conformations of the insulin subunit. Herein, the 2Zn form will be referred to as T_6, the 4Zn form as T_3R_3, and the phenol-induced form as R_6.[2]

Several groups have reported evidence indicating that the interconversion of the extended (T) and helical (R) conformations of the B-chain takes place in solution (Bentley et al., 1975; Williamson & Williams, 1979; Renscheidt et al., 1984; Ramesh & Bradbury, 1986; Palmieri et al., 1987; Wollmer et al., 1987).[3] These studies show that the insulin hexamer exhibits distinctly different spectroscopic properties under T_6, T_3R_3, and R_6 conditions. While there are no solution structures available, we believe it is reasonable to expect that under T_6 and R_6 conditions the hexamer structures are essentially the same as the crystalline T_6 and R_6 forms, respectively. The existence of a T_3R_3 form in solution seems to be on a less firm basis. The crystallographers have proposed that the hexamer is constrained to the T_3R_3 state by crystal lattice forces (Smith et al., 1984). Ramesh and Bradbury (1986) interpret their NMR data in the presence of SCN^- as evidence for the T_3R_3 form in solution, while Palmieri et al. (1988) found no compelling evidence for a T_3R_3 structure (but did not eliminate this possibility) and therefore proposed SCN^- gives an R_6 structure in solution.

In previous work from this laboratory (Dunn et al., 1980; Storm & Dunn 1985; Kaarsholm & Dunn, 1987), the planar tridentate chelators 2,2′,2″-terpyridine (terpy) and 4-(2-pyridylazo)resorcinol (PAR) have been used in combination with UV–visible spectroscopy and rapid kinetic methods to characterize the microenvironment of zinc ion and the kinetics

[2] This nomenclature can be expanded to describe the small differences in conformation of insulin monomers within the dimeric unit of the 2Zn or phenol-induced forms by designating these forms T and T′ and R and R′, respectively. Accordingly, the crystalline 2Zn hexamer then would be a $T_3T'_3$ species and the phenol-induced species would be an $R_3R'_3$ species.

[3] Our unpublished ^1H FT NMR studies (M. Roy, R. W.-K. Lee, N. C. Kaarsholm, and M. F. Dunn, in preparation) show that in solution SCN^- does not convert all insulin subunits to the R form, whereas the transformation is complete in the presence of phenol.

of dissociation of the insulin hexamer, $(In)_6(Zn^{2+})_2$, under T_6 conditions. In the present work, we exploit the chromophoric chelator approach to probe the SCN^--induced transition in solution, and we compare the chelator-induced dissociation kinetics of insulin, proinsulin, and miniproinsulin. Miniproinsulin is a single-chain insulin derivative with partially reduced flexibility due to a dipeptide cross-linkage between Gly-A1 and Ala-B30. Like proinsulin, this species is essentially biologically inactive (Markussen et al., 1987). The results show the three proteins exhibit closely similar kinetics of chelator-induced dissociation under T_6 conditions. All three species are found to undergo a T to R transition in solution, and the kinetics of dissociation under T_3R_3 conditions are shown to be quantitatively the same for the three proteins. In contrast, the sequestering and removal of Zn^{2+} under R_6 conditions is an extremely slow process.

Materials and Methods

Materials. Porcine insulin, porcine proinsulin (Steiner et al., 1968; Snel & Damgaard, 1988), and B(1–30)-Ala-Lys-A(1–21) porcine insulin, i.e., a miniproinsulin (Markussen et al., 1987), were prepared at the Novo Research Institute. In some of the experiments, porcine insulin from the Elanco Division of Eli Lilly was used. KSCN and phenol (analytical grade) were obtained from Mallinckrodt and Aldrich, respectively. The sources of all other materials have been given elsewhere (Dunn et al., 1980; Storm & Dunn, 1985; Kaarsholm & Dunn, 1987).

Methods. Metal-free protein stock solutions with a $[Zn^{2+}]/[P]$ ratio of less than 0.003 were prepared by treatment of samples with Chelex 100 resin as previously described for insulin (Dunn et al., 1980). The same extinction coefficient, $\epsilon_{276} = 6.1 \times 10^3\ M^{-1}\ cm^{-1}$, was used for the determination of the concentration of each monomer species (Frank & Veros, 1968). Values of extinction coefficients for PAR, terpy, and their metal complexes as well as procedures for preparation of metal–protein solutions and spectrophotometric quantitation of metal ion content have been described (Dunn et al., 1980; Storm & Dunn, 1985; Kaarsholm & Dunn, 1987). Single-wavelength, rapid kinetic measurements and the kinetic analyses were carried out with a Durrum stopped-flow apparatus and computerized data acquisition system as described by Dunn et al. (1979). The absorbance vs time data were fitted to a sum of exponentials, $\sum_i \Delta OD_i \exp(t/\tau_i)$, where ΔOD_i and τ_i are the amplitudes and corresponding relaxation times, respectively, employing the minimum number of phases necessary to reconstruct the experimental time course without systematic deviation. All kinetic experiments were carried out in 0.05 M Tris-HCl buffer, pH 8.0. Typical observation wavelengths were 333 nm for terpy reactions and 530 nm for PAR reactions.

For the solution work presented in this paper, we define T_6 conditions as Tris-HCl buffer, pH 8.0. With the same buffer system, T_3R_3 and R_6 conditions are defined respectively as $[SCN^-] > 30$ mM and [phenol] > 10 mM. These SCN^- and phenol concentrations are sufficient for the formation of the T_3R_3 and R_6 crystal forms (albeit at different pH), and these concentrations are sufficient to saturate those changes in the insulin ^1H NMR spectrum that characterize the effects of these ligands[3] (M. Roy, R. W.-K. Lee, N. C. Kaarsholm, and M. F. Dunn, unpublished results).

Results

Kinetics of Chelator-Induced Dissociation under T_6 Conditions. The reference system for the present work is the reaction between zinc–insulin and a variable excess of a

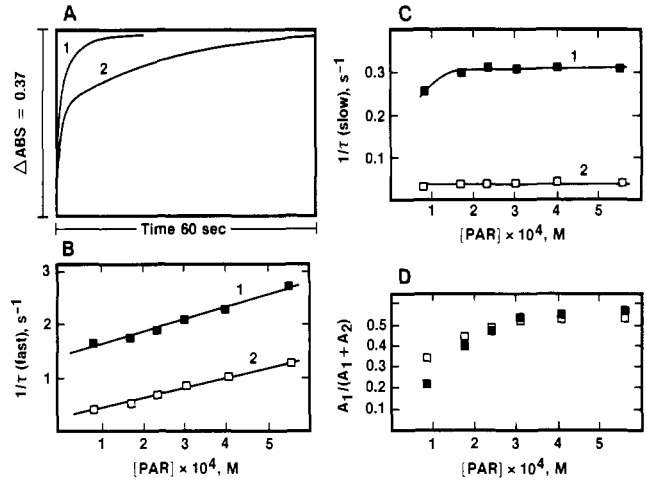

FIGURE 1: Effect of 50 mM SCN^- on the biphasic kinetics of the sequestering and removal of Zn^{2+} from the insulin hexamer by a large excess of PAR at pH 8.0. Reaction was initiated by rapidly mixing insulin preincubated with Zn^{2+} ($[Zn^{2+}]/[In] = 0.2$) with a variable excess of PAR in the absence (●) or presence (□) of 50 mM SCN^-. Conditions after mixing: [In], 50 μM; $[Zn^{2+}]$, 10 μM; [PAR], variable; 25 ± 0.2 °C. Absorbance changes were followed at 530 nm. Panel A shows representative stopped-flow traces with 560 μM PAR in the absence (trace 1) or presence (trace 2) of 50 mM SCN^-. Panels B, C and D show the concentration dependencies of, respectively, the observed rates of the two relaxations and the relative amplitudes of the two phases. The best-fit straight lines in (B) yield slopes and intercepts of $2.3 \times 10^3\ M^{-1}\ s^{-1}$ and $1.4\ s^{-1}$ in the absence of SCN^- and $1.8 \times 10^3\ M^{-1}\ s^{-1}$ and $0.26\ s^{-1}$ in the presence of 50 mM SCN^-. The saturated value of the slow relaxation rate constant (C) is $0.32\ s^{-1}$ in the absence of SCN^- and $0.05\ s^{-1}$ in the presence of 50 mM SCN^-.

chromophoric tridentate chelator, i.e., PAR or terpy. This reaction leads to the sequestering and ultimate removal of all the insulin-bound Zn^{2+} (Dunn et al., 1980; Kaarsholm & Dunn, 1987).

As shown in Figure 1A (trace 1), the time course for the appearance of the zinc–chelator complexes is characterized by two poorly separated relaxations of roughly equal amplitude. The rate of the faster process increases linearly with increasing concentration of chelator, while the rate of the slower process first increases and then saturates as the concentration of chelator is raised (compare curve 1 of Figure 1B with curve 1 of Figure 1C).

A minimum mechanism that encompasses this behavior has previously been proposed (Dunn et al., 1980). The scheme postulates the fast coordination of chelator (che) to the protein-bound zinc ion (eq 1) followed by the slow, rate-limiting dissociation of chelator-bound zinc ion from the protein (P) (eq 2) and the rapid coordination of a second chelator molecule to give the bis complex $(che)_2Zn^{2+}$ (eq 3):

$$che + (H_2O)_3Zn^{2+}P \overset{fast}{\rightleftharpoons} (che)Zn^{2+}P + 3H_2O \quad (1)$$

$$(che)Zn^{2+}P \overset{slow}{\rightleftharpoons} (che)Zn^{2+} + P \quad (2)$$

$$che + (che)Zn^{2+} \overset{fast}{\longrightarrow} (che)_2Zn^{2+} \quad (3)$$

Kinetics of Chelator-Induced Dissociation under T_3R_3 Conditions. The effect of 50 mM SCN^- on the dissociation kinetics is shown in Figure 1. The reaction still leads to the ultimate removal of all the insulin-bound Zn^{2+} in a biphasic process (trace 2 of Figure 1A), but the rates of both phases are reduced (compare parts B and C of Figure 1). The rate of the faster phase still increases linearly with [PAR]. The major difference is a pronounced reduction in the rate of the slow phase (Figure 1C). The value of the *Y*-axis intercept in the plot of $1/\tau$ (fast) vs [PAR] is reduced, but the slope of

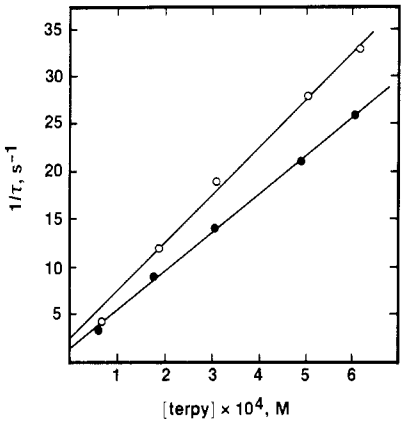

FIGURE 2: Concentration dependence of the observed rate constant of the relaxation for the monophasic reaction between Cd^{2+}–insulin and a variable excess of terpy at pH 8.0. Conditions after mixing: [In], 37.5 μM; [Cd^{2+}], 7.5 μM; [terpy], variable; in the absence (●) or presence (○) of 50 mM SCN^-. The best-fit straight lines yield slopes and intercepts of 4.0×10^4 M^{-1} s^{-1} and 1.47 s^{-1} in the absence of SCN^- and 5.0×10^4 M^{-1} s^{-1} and 2.46 s^{-1} in the presence of 50 mM SCN^-.

the plot is almost unchanged (Figure 1B). The rate of the slow process is reduced almost 10-fold and appears to be zeroth order in PAR over the full concentration range (Figure 1C). Finally, Figure 1D shows that SCN^- has little if any effect on the relative amplitudes of the two phases. Under both sets of conditions at low [PAR], the fraction of the total OD change occurring in the fast phase increases with increasing [PAR] and then approaches a saturating value of about 0.55 at high concentrations. The change in rate behavior is not simply an ionic strength effect due to 50 mM SCN^-. The behavior under T_6 conditions (Figure 1) is unaffected by Cl^- ion concentrations ranging from 2.5 to 100 mM. [The Cl^--ion induced conversion of T_6 to T_3R_3 in the crystalline state requires much higher concentrations >0.3 M (De Graaf et al., 1981).] However, 200 mM I^- gives kinetics similar to those observed in 50 mM SCN^- (Kaarsholm and Dunn, unpublished results).

Substitution of divalent cations for Zn^{2+}, i.e., Cd^{2+}, Cu^{2+}, and Ni^{2+}, prevents the SCN^--induced T_6 to T_3R_3 structural transformation in insulin crystals (De Graff et al., 1981). Therefore, to establish that the effect of SCN^- observed in Figure 1 is a true reflection of the SCN^--induced conformation state, Zn^{2+} was substituted with Cd^{2+} in the kinetic experiments. Figure 2 shows the effect of 50 mM SCN^- on the kinetics of the reaction between cadmium–insulin and a variable but large excess of terpy. In contrast to the zinc–insulin system, this reaction is monophasic, and the apparent rate constant for this relaxation increases linearly with [terpy]. Apparently, the ternary complex with Cd^{2+} predicted by eq 1–3 is not sufficiently stable to accumulate during the reaction.[4] However, as clearly shown in Figure 2, 50 mM SCN^- has no significant effect on the kinetics of the reaction.

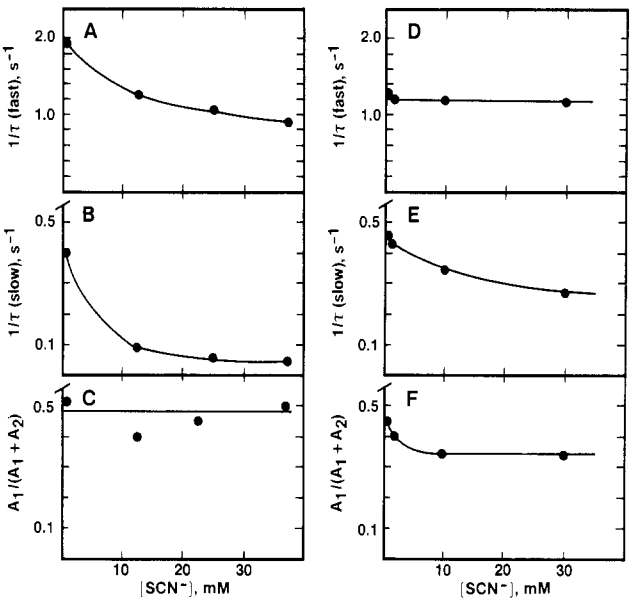

FIGURE 3: Concentration dependence of the effect of SCN^- on the kinetics of the reactions between PAR and zinc–insulin at pH 8.0. For panels A–C conditions after mixing are 50 μM insulin, 10 μM Zn^{2+}, and 290 μM PAR; i.e., [PAR] ≫ [Zn^{2+}]. For panels D–F conditions after mixing at 250 μM insulin, 50 μM Zn^{2+}, and 5 μM PAR; i.e., [Zn^{2+}] ≫ [PAR]. In all cases, biphasic kinetics are observed. Panels A and D show the effect of increasing [SCN^-] on the fast relaxation rate constant, panels B and E show the effect on the slow relaxation rate constant, and panels C and F show the effect on the amplitude ratio.

The concentration dependence of the SCN^- effect was studied under two sets of conditions. In the first set of conditions, the effect of increasing [SCN^-] on the kinetics of the biphasic reaction between zinc–insulin and a fixed excess of PAR was investigated (Figure 3A–C). Both rates decrease significantly with increasing [SCN], while the amplitude ratio remains essentially constant. These results are in accord with those presented in Figure 1 and show that the effect on both rates saturates at about 30 mM SCN^-. The fact that the same concentration of SCN^- is required for the 2Zn to 4Zn insulin transformation in the crystal (De Graaff et al., 1981) further underscores the equivalence between these kinetic phenomena and the observations made in the crystalline state (Smith et al., 1984; Bentley et al., 1976).

In the second set of conditions, the effect of increasing [SCN^-] on the kinetics of the biphasic reaction between PAR and a fixed excess of zinc–insulin was studied (Figure 3D–F). The fast rate is independent of [SCN^-], the slow rate decreases slightly (but not to the level observed in Figure 3B), and the amplitude ratio is nearly independent of [SCN^-]. These data show that in the presence of SCN^- there is still a protein-bound zinc species that reacts according to eq 1–3. In the absence of SCN^-, it has previously been shown that the concentration dependencies of the relaxation rates and relative amplitudes for the reaction between PAR and zinc–insulin are similar regardless of whether $[PAR]_0 \gg [Zn^{2+}]_0$ or $[PAR]_0 \ll [Zn^{2+}]_0$ (Kaarsholm & Dunn, 1987). Therefore, although the fraction is substantial, it is not possible from the data of Figure 3D–F to estimate the fraction of the total Zn^{2+} that reacts according to eq 1–3 in the presence of a high concentration of SCN^-.

Comparison of Zinc Binding Domains for the Insulin, Proinsulin, and Miniproinsulin Hexamers via Reaction with terpy. The properties of the high-affinity Zn^{2+} binding sites, of insulin, proinsulin, and miniproinsulin hexamers were

[4] The observation of monophasic kinetics for the reaction between terpy and the cadmium–insulin system is at variance with the previously published findings of Storm and Dunn (1985). The experiment shown in Figure 2B of that paper employed [Cd^{2+}] = 4.8 μM and [In] = 75 μM, i.e., [Cd^{2+}]/[In] = 0.064. Biphasic kinetics were observed with a second-order rate constant, 4×10^4 M^{-1} s^{-1} for the fast phase, identical with that found in Figure 2 of this work. The relative amplitude of the slow phase was found to constitute about 20% of the total OD change. A Zn^{2+} contamination of the insulin solution corresponding to [Zn^{2+}] ≃ 1–2 μM and [Zn^{2+}]/[In] ≃ 0.01–0.03 most likely produced the slow phase they observed. In the present work employing [Cd^{2+}] = 7.5 μM and [In] = 20–150 μM, we have found no evidence for biphasic kinetics in the reaction with excess terpy (data not shown).

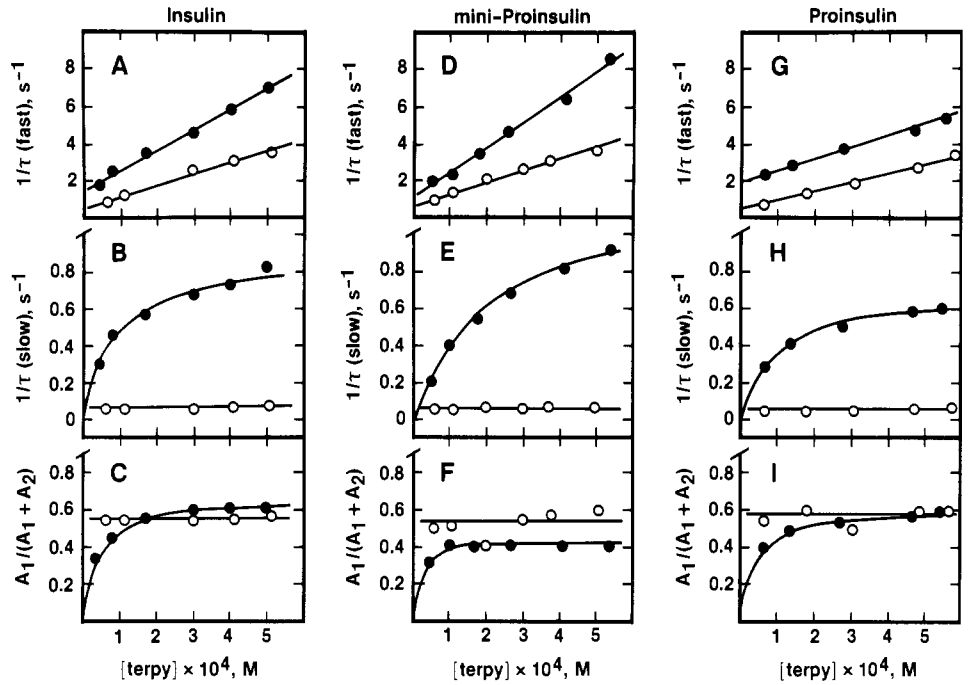

FIGURE 4: Comparison of concentration dependencies of the relaxation rate constants and relative amplitudes for the biphasic reactions of terpy with zinc complexes of insulin (A–C), miniproinsulin (D–F), and proinsulin (G–I) in the absence (●) or presence (○) of 50 mM SCN^- at pH 8.0. Conditions after mixing: [P], 37.5 μM; [Zn^{2+}], 7.5 μM; [terpy], variable. The straight lines and hyperbolas are drawn by using the parameters listed in Table I.

Table I: Summary of Relaxation Kinetic Data for the Reactions of the Insulin, Proinsulin, and Miniproinsulin Hexamers with terpy both in the Absence and in the Presence of SCN^- at pH 8.0

	T_6 conditions[a]							T_3R_3 conditions[b]				
protein	$k_1 \times 10^{-4}$ (M^{-1} s^{-1})	k_{-1} (s^{-1})	$k_2$max (s^{-1})	k_{-1}/k_1 (μM)	$K_{0.5}$ (μM)	A_1max/($A_1 + A_2$)	$A_{0.5}$ (μM)	$k_1 \times 10^{-4}$ (M^{-1} s^{-1})	k_{-1} (s^{-1})	k_2 (s^{-1})	k_{-1}/k_1 (μM)	$A_1/(A_1 + A_2)$
insulin	1.09	1.46	0.8	134	71	0.68	39	0.56	0.50	0.05	89	0.56
proinsulin	0.56	1.90	0.7	339	95	0.61	34	0.48	0.40	0.05	83	0.55
miniproinsulin	1.35	1.06	1.4	79	264	0.46	25	0.64	0.55	0.05	86	0.58

[a] Best-fit parameters assuming a linear dependence of $1/\tau$(fast) and a hyperbolic dependence of $1/\tau$(slow) and of the amplitude ratio, $A_1/(A_1 + A_2)$, i.e., $1/\tau(\text{fast}) = k_{-1} + k_1[\text{terpy}]$, $1/\tau(\text{slow}) = k_2\text{max}\,[\text{terpy}]/(K_{0.5} + [\text{terpy}])$, and $A_1/(A_1 + A_2) = [(A_1\text{max}/(A_1 + A_2)][\text{terpy}]/(A_{0.5} + [\text{terpy}])$; cf. eq 1–3. [b] In the presence of 50 mM SCN^-, $1/\tau(\text{fast}) = k_{-1} + k_1[\text{terpy}]$, while both $1/\tau(\text{slow}) = k_2$ and $A_1/(A_1 + A_2)$ are zeroth order in terpy over the range of concentrations studied; cf. eq 4.

compared by reaction with terpy under conditions where $[Zn^{2+}]/[P] \leq 0.3$ and $[\text{terpy}]_0 \gg [Zn^{2+}]_0$. For all three protein species, the terpy absorbance changes characterizing this reaction are biphasic. Figure 4 shows the dependencies of the amplitudes and apparent rate constants of the two relaxations for each protein system as a function of increasing concentration of terpy. The quantitative rate data summarized in Table I indicate a striking similarity between the kinetic parameters for the three proteins. For each species the rate of the fast relaxation is proportional to [terpy], while the rate of the slow relaxation is proportional to [terpy] at low concentrations but tends toward a limiting (saturated) value at high [terpy]. In each case, the fraction of the total absorbance change that takes place in the fast relaxation increases and then saturates at a value of about 0.4–0.7 (Table I). Thus, the kinetic behavior is consistent with mechanisms that involve a fast bimolecular step that is coupled to a slower, first-order process (e.g., eq 1–3). The data presented in Figure 4 and Table I indicate this mechanism is a common feature of the insulin, proinsulin, and miniproinsulin hexamers.

The dependence of the rates and relative amplitudes of the terpy reaction on the $[Zn^{2+}][P]$ ratio was investigated in experiments where a fixed excess of terpy is reacted with Zn^{2+} premixed with variable amounts of either insulin, proinsulin, or miniproinsulin (Table I). As exemplified for insulin in Figure 5, for the three proteins, the results obtained are closely similar.

When the $[Zn^{2+}]/[P]$ is ≤0.3, the observed time courses are biphasic and the ratio of the amplitudes $A_1/(A_1 + A_2) \simeq 0.5$. The relaxation rate constants for the two phases are invariant. For $[Zn^{2+}]/[P]$ ratios >0.3, the observed time courses are triphasic. The relaxation rate constant of the first phase of the triphasic time course is at least 10-fold greater than that of the second phase (data not shown). The relaxation rates and relative amplitudes associated with the second and third phases correspond to those of the biphasic time courses obtained when $[Zn^{2+}]/[P] \leq 0.3$ (Figure 5A–C; Table I). As the $[Zn^{2+}]/[P]$ ratio is raised above 0.3, there is a marked increase in the fraction of the fastest reacting Zn^{2+} species. These results show that the stoichiometry of high-affinity zinc binding is the same for the three proteins and that under these conditions the reactivity of the zinc–protein species is largely insensitive to variations of the $[Zn^{2+}]/[P]$ ratio below 0.3.

Comparison of Structural Flexibility for Insulin, Proinsulin, and Miniproinsulin. Under conditions where $[Zn^{2+}]/[P] \leq 0.03$ and $[\text{terpy}]_0 \gg [Zn^{2+}]_0$, the effect of 50 mM SCN^- on the kinetics of chelator-induced dissociation was compared for the three protein species. As shown in Figure 4, the effects on proinsulin and miniproinsulin are very similar to those observed for insulin. Each reaction is biphasic and the rates

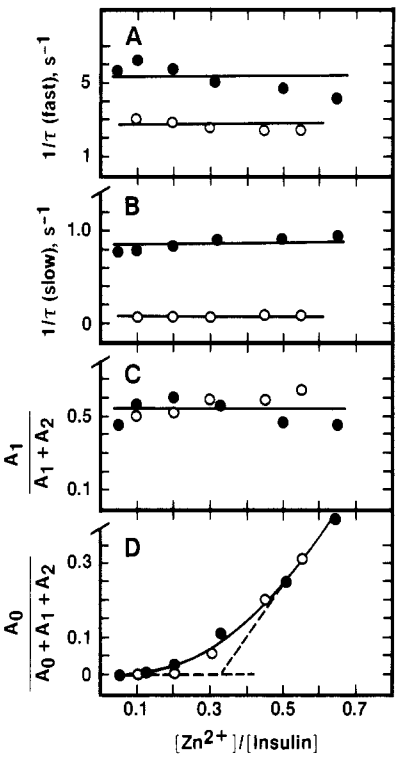

FIGURE 5: Dependence on the $[Zn^{2+}]/[In]$ ratio of relaxation rate constants (A and B) and relative amplitudes (C) for the biphasic time courses characterizing the reaction of terpy with the zinc–insulin system in the absence (●) or presence (○) of 50 mM SCN^- at pH 8.0. When the $[Zn^{2+}]/[In]$ ratio is >0.3, the time courses become triphasic and the relative amplitude, $A_0/(A_0 + A_1 + A_2)$, of this new, fastest phase increases with increasing $[Zn^{2+}]/[In]$ (panel D). Conditions after mixing: [terpy], 360 μM; $[Zn^{2+}]$, 10 μM; [In], variable (●). Conditions in the presence (○) of SCN^-: [terpy], 400 μM; $[Zn^{2+}]$, 7.5 μM; [In], variable.

of the fast relaxations increase linearly with [terpy]. The effect of SCN^- on the plot of $1/\tau$ (fast) vs [terpy] is a slight reduction in slope and a decrease in the y-axis intercept (Figure 4A,D,G; Table I). The rates of the slow relaxations are greatly reduced in the presence of SCN^- and in each case appear to be zeroth order in terpy over the full concentration range investigated (Figure 4B,E,H; Table I). As is the case also for insulin, SCN^- has essentially no effect on the amplitude ratio, $A_1/(A_1 + A_2)$, for either proinsulin or miniproinsulin (Figure 4C,F, and I). The quantitative rate data are summarized in Table I. These results show that insulin, proinsulin, and miniproinsulin all undergo conformational transitions in solution when conditions are changed from T_6 to T_3R_3, and the transformation results in nearly identical changes of zinc ion environment for each of the three hexamers.

The effect of 50 mM SCN^- is compared for the three proteins under conditions where a fixed excess of terpy is reacted with Zn^{2+} premixed with variable amounts of protein. Again, the dependence of rates and relative amplitudes on the $[Zn^{2+}]/[P]$ ratio is closely similar for each of the three proteins (the results for insulin are presented in Figure 5 for illustration).

Just as is observed in the absence of SCN^-, at values of the $[Zn^{2+}]/[P]$ ratio >0.3, the observed time courses are biphasic and the ratio of amplitudes and the relaxation rate constants for the two phases are invariant. For values of the $[Zn^{2+}]/[P]$ ration >0.3, a new, faster phase is detected and the time courses become triphasic. The fraction of Zn^{2+} reacting in the first phase of the triphasic time courses increases (Figure 5D), while the relaxation rate constants and the amplitudes of the second and third phases (viz., Figure 5C) remain essentially constant. Consequently, it appears that *under both T_6 and T_3R_3 conditions, the critical stoichiometry for the interaction between Zn^{2+} and each of the three protein species is two per hexamer.* Also under T_3R_3 conditions, the reactivity of the zinc–protein species is essentially insensitive to variations of the $[Zn^{2+}]/[P]$ ratio in the range below 0.3.

Reaction of terpy with the Zinc–Insulin Hexamer under R_6 Conditions. The reaction of terpy with solutions of zinc–insulin containing phenol under conditions similar to those required to form the crystalline R_6 hexamer was studied as a function of the concentrations of phenol and terpy. The rate of the sequestering and removal of insulin-bound zinc ion is monophasic and extremely slow in comparison to rates measured under T_6 and T_3R_3 conditions (data not shown). For example, when 250 μM terpy is reacted with a mixture of 50 μM insulin and 10 μM Zn^{2+} in the presence of 0.053 M phenol at pH 8.0, a rate of 8×10^{-4} s^{-1} was measured.[5]

Discussion

The X-ray structure of the T_6 conformation shows that the hexamer has two identical faces at each end of the cylindrical structure (Baker et al., 1988). Each face is a broad shallow depression that contains Zn^{2+} coordinated by three His-B10 imidazole groups and three water molecules in a distorted octahedral ligand field. The water molecules point out into the depression and are exposed to the environment. This geometry is consistent with a mechanism for sequestering and removal of Zn^{2+} in which the water molecules are exchanged for chelators such as terpy or PAR which then remove the Zn^{2+} and initiate dissociation. The T_3R_3 structure has two different faces. One face is identical with that found in the T_6 structure because three of the six B-chains retain the extended B1–B8 conformation. As a result of the helical (B1–B19) conformation of the amino termini of the other three B-chains, the second face is filled in by three α-helices related by the 3-fold axis (Smith et al., 1984). At the zinc site located on the 3-fold axis at this end of the hexamer, the three water molecules are replaced by a single, buried ligand (either a water molecule or the lyotropic ion). This structural motif predicts that the buried ligand is protected from replacement by chelators such as terpy since the only obvious access to the ligand is by traversing a narrow tunnel 8 Å long with dimensions too small to accommodate PAR or terpy (Smith et al., 1984). In the R_6 structure, all six insulin subunits have the helical B1–B19 structure and both faces are filled in by these helices. Hence, both of the axial Zn^{2+} sites are buried.

In the discussion that follows, our working assumption is that in solution T_6 and R_6 conditions give hexamer conformations analogous to the T_6 and R_6 crystal structures. This assumption is fully consistent with all the published studies of which we are aware that have relevance to the solution structures of the insulin hexamer under T_6 and R_6 conditions (Williamson & Williams, 1979; Renscheidt et al., 1984; Wollmer et al., 1987).

As a first result of the present investigation, the kinetic data obtained under T_6 conditions show that neither the substantial increase in hydrophilicity due to the 33 residue C-peptide in proinsulin nor the restricted flexibility imposed by the dipeptide cross-linkage in miniproinsulin affects the microenvironment of Zn^{2+} bound to the high-affinity sites in these hexamers. Hence, the decisive factors limiting the rates of the chela-

[5] After the completion of the present work, we have been informed by A. Wollmer (private communication) that his laboratory has made an independent observation that reaction of another tridentate chelator with the zinc–insulin hexamer is similarly slowed by the presence of *m*-cresol.

tor-mediated removal of the Zn^{2+} and hexamer dissociation are fundamental properties of the A- and B-chain portions of the insulin molecule. This conclusion accords well with previously published data. Equilibrium dialysis zinc binding studies and sedimentation equilibrium measurements have shown that both insulin and proinsulin aggregate to form soluble hexamers in the presence of limited amounts of Zn^{2+} (Grant et al., 1972; Frank et al., 1972). Similarly, comparative X-ray diffraction studies of insulin and the cross-linked derivative A1–B29-diaminosuberoylinsulin, have shown that the A- and B-chains of insulin and of the cross-linked derivative have essentially the same structure (Cutfield et al., 1981).

The observation that the kinetic parameters (Figures 1–5, Table I) respond similarly to variations in the $[Zn^{2+}]/[P]$ ratio under both T_6 and T_3R_3 conditions is of considerable importance to the present work. The invariance of rates and amplitudes for $[Zn^{2+}]/[P] \leq 0.3$ and the appearance of an additional fast kinetic phase when $[Zn^{2+}]/[P] > 0.3$ (viz., Figure 5) strongly suggest that under both sets of conditions the predominant species is a hexamer containing two tightly bound zinc ions. Since any Zn^{2+} residing in the off-axial sites of the 4Zn structure would be expected to exhibit reduced reactivity toward chelators and since the additional fast phase appears in a similar manner under both T_6 and T_3R_3 conditions, we conclude that off-axial coordination in the T_3R_3 structure is of minor importance in solution.[6] In accordance with this result, Renscheidt et al. (1984) found that SCN^- induces similar changes in the circular dichroism spectra of insulin and an insulin mutant in which His-B5 has been replaced by Ala; hence, Zn^{2+} binding to the off-axial coordination sites is not essential to the conformational transition.

A number of previous studies have dealt with the question of symmetry in the T_6 and T_3R_3 structures. The small differences between monomers in T_6 insulin are probably the result of interhexamer contacts within the crystal lattice (Chothia et al., 1983). In T_3R_3 insulin crystals, hexamers move 0.36 nm further apart in the direction of the crystal *c* axis. As a consequence, the much greater differences between monomers in this structure are difficult to separate from concomitant changes in hexamer/hexamer interactions (Bentley et al., 1978). It is possible that the differences found between monomers of the crystalline T_3R_3 insulin hexamer disappear in solution. Williamson and Williams (1979) in their ^1H NMR analysis argued that since SCN^- causes half of the tyrosines to undergo a chemical-shift change, the SCN^--induced structure is symmetrical in solution. Ramesh and Bradbury (1986), on the other hand, resolved the histidine C-2 proton region of the NMR spectra into four separate resonances and concluded that the T_3R_3 (as well as the T_6) structures are asymmetric in solution. However, a more recent study (Palmieri et al., 1988) indicates the conditions used by Ramesh and Bradbury (1986) result in incomplete assembly of hexamers and that the His C-2 proton resonances they observed do not originate from a homogeneous preparation of insulin species. Palmieri et al. (1988) found that in the presence of SCN^- the His-B5 and His-B10 C-2 protons of hexameric insulin exhibit single broad resonances, thus providing no evidence for asymmetry. Therefore, it is unclear whether or not the T_3R_3 structure is a significant species in solution under T_3R_3 conditions.[3] Nevertheless, the solution behavior of the hexamer under T_3R_3 conditions is distinctly different from that found for either T_6 or R_6 conditions.

To limit discussion of mechanism, we assume that in solution both SCN^- and phenol mediate conformational transitions in which some or all insulin subunits undergo the B1–B9 extended chain to helix conformation change (i.e., the T or R transition). There are at least four plausible types of T to R mechanisms consistent with the rate, amplitude, and stoichiometry measurements reported in Table I and Figures 1–5 for the SCN^--mediated transition. These four are a subset from the general mechanism for ligand-induced conformation changes proposed by Eigen (1967).

Mechanisms Involving either Concerted or Stepwise T_6 to R_6 Transitions. (*a*) When applied to the insulin hexamer, the concerted model (Monod et al., 1965) proposes that only the T_6 and R_6 conformations exist in solution (eq 4, where *n* is

$$\begin{array}{ccc} T_6 & \rightleftharpoons & R_6 \\ {\scriptstyle SCN^-}\downarrow\uparrow & & \uparrow\downarrow{\scriptstyle SCN^-} \\ T_6(SCN^-)_1 & \rightleftharpoons & R_6(SCN^-)_1 \\ {\scriptstyle SCN^-}\downarrow\uparrow & & \uparrow\downarrow{\scriptstyle SCN^-} \\ \vdots & & \vdots \\ {\scriptstyle SCN^-}\downarrow\uparrow & & \uparrow\downarrow{\scriptstyle SCN^-} \\ T_6(SCN^-)_n & \rightleftharpoons & R_6(SCN^-)_n \end{array} \qquad (4)$$

the stoichiometry of SCN^- binding sites). Provided SCN^- binds both to T_6 and to R_6, it is possible that in the presence of *saturating* SCN^- solutions of all three hexamers (i.e., insulin, proinsulin, and miniproinsulin) contain roughly equal amounts of the T_6 and R_6 conformations. The fast relaxation obtained in the presence of saturating SCN^- is roughly the average of the two, poorly resolved relaxation rate constants observed under T_6 conditions. The biphasicity in the reaction time courses then would reflect a situation where the fast phase is due to reaction of the T_6 species via the poorly resolved steps of eq 1–3, and the slow phase is due to reaction of R_6 via a rate-limiting interconversion of R_6 to T_6 followed by eq 1–3.

(*b*) The sequential model of Koshland et al. (1966) is usually presented as an alternative to the concerted model. One variation of this model that depicts the distribution of R and T states in the presence of saturating SCN^- is

$$(SCN^-)_6T_6 \overset{K_1}{\rightleftharpoons} (SCN^-)_5T_5R_1(SCN^-)_1 \overset{K_2}{\rightleftharpoons} \cdots \overset{K_5}{\rightleftharpoons} (SCN^-)_1T_1R_5(SCN^-)_5 \overset{K_6}{\rightleftharpoons} R_6(SCN^-)_6 \qquad (5)$$

Due to the large number of states described by eq 5, it is difficult to discuss all of the possible distributions of species that might explain the biphasicity, amplitudes, and stoichiometry of the terpy reaction in the presence of saturating SCN^-. Furthermore, it is not entirely obvious how species such as $(SCN^-)_5T_5R_1(SCN^-)_1$ or $(SCN^-)_4T_4R_2(SCN^-)_2$ would bind Zn^{2+}. Clearly, a distribution dominated by roughly equal amounts of $(SCN^-)_6T_6$ and R_6 $(SCN^-)_6$ (viz., the preceding discussion) could explain the data, as could a distribution dominated by $(SCN^-)_3T_3R_3(SCN^-)_3$ (see the following dis-

[6] The T_3R_3 X-ray structure (Smith et al., 1984) is for the hexamer crystallized in the presence of high NaCl concentrations. At each (partially occupied) off-axial site zinc coordinates two solvent or lyotropic ligands; the axial tetrahedral site coordinates one. Although the T_6 to T_3R_3 conversion could, in principle, bring about a change in the number of Zn^{2+} sites from 2 to 4, the T_3R_3 crystal structure shows a total occupancy of only 2.67 Zn^{2+}/hexamer (Smith et al., 1984). It is possible that the discrepancy (if one exists) between the stoichiometry of $2Zn^{2+}$/hexamer found in these kinetic studies and the total Zn^{2+} occupancy value of 2.67 reported for the X-ray structure is due to the use of SCN^- in place of Cl^- to induce the conformation change. If for steric and/or electronic reasons SCN^- stabilizes the axial tetrahedral site, then the T_3R_3 conformation would have only two high-affinity zinc sites. Therefore, although other explanations are possible (see text), the amplitude dependencies shown in Figure 5 are in reasonable agreement with the postulation of a T_3R_3 structure in solution.

cussion). The disadvantages of both the concerted and the sequential proposals stem from the coincidences that must be envoked (i.e., the thermodynamics of SCN^- binding either must make the stabilities of the T_6 and R_6 states roughly equal for insulin, proinsulin, and miniproinsulin or binding must stabilize a T_3R_3 species relative to all others).

Mechanisms That Involve a T_3R_3 Species. (*a*) One mechanism in this class assumes that the two axial Zn^{2+} ions of the SCN^--induced structure behave identically. This type of reactivity has been shown to be consistent for the zinc hexamer obtained under T_6 conditions (see Figure 4; eq 1–3; Dunn et al., 1980; Kaarsholm & Dunn, 1987). If this mechanism also is operative under T_3R_3 conditions, then formation of a ternary complex at each protein-bound Zn^{2+} site occurs in much the same way as is observed in the absence of SCN^-. The effect of SCN^- is then expressed as a stabilization of the ternary complex leading to a greatly reduced rate of dissociation of the (che)Zn^{2+} species. This mechanism is qualitatively consistent with most of the kinetic data, but not with the T_3R_3 crystal structure. The results presented in Figure 3D–F would need be explained by incomplete transformation of all zinc ion environments in the presence of 30 mM SCN^- (a concentration that saturates the kinetic effect).

(*b*) An attractive mechanistic alternative involves the existence of T_3R_3 species with two types of axial Zn^{2+} in the presence of SCN^-. Such a structure exists in crystalline T_3R_3 (Smith et al., 1984). A number of observations in solution are consistent with this view. In this mechanism, the fast process in the terpy reaction would represent the sequestering and complete removal of Zn^{2+} from essentially unchanged microenvironments in two poorly resolved steps (eq 1–3). This interpretation immediately explains the results of Figure 3D–F. The slow process under T_3R_3 conditions then would represent the reaction of a new class of zinc ion microenvironments[6] induced by SCN^-. Accordingly, the rate of this slow process would be zeroth order in che over the full concentration range (cf. parts B, E, and H of Figure 4). The observation that approximately half of the total OD change occurs in each phase in both the absence or the presence of SCN^- (Figures 1C, 3C, and 4C,F,I) then has two different origins. Under T_6 conditions, half of the OD change is due to the formation of a ternary complex at each protein-bound Zn^{2+} (eq 1–3; Dunn et al., 1980). Under T_3R_3 conditions, the OD change observed in the fast phase represents the complete removal of approximately half of all protein-bound Zn^{2+} in a process that is the net reaction of eq 1–3. In this case, the amplitude ratio indicates that about half of the bound zinc ion resides in an environment little affected by SCN^-, while the other half is transformed to a state that is inaccessible to che.

It follows that the slow relaxation observed under T_3R_3 conditions would include contributions from the reversal of the protein conformation to the T_6 state. This protein conformational change would make the remaining Zn^{2+} ion accessible to reaction with the chelator as shown in

$$T_3R_3 \underset{}{\overset{\geq 0.05\ s^{-1}}{\rightleftharpoons}} T_6 + \text{che} \rightarrow \text{eq 1–3} \qquad (6)$$

The highly similar kinetics observed for hexamers of insulin, proinsulin, and miniproinsulin show that these proteins all assume highly similar conformations in the presence of SCN^- and that the rate-limiting step for the dissociation of these forms is the same in each case. This result extends the observation made by Renscheidt et al. (1984) that SCN^- induces similar changes in the CD spectra of insulin and another miniproinsulin, i.e., the A1–B29-diaminosuberoyl derivative of insulin. The in vivo role of the T to R transition is unknown, but for modified insulins, the ability to undergo the transition has been considered essential for the efficient expression of biological activity (Dodson et al., 1983).

The finding that under conditions similar to those required for the formation of crystalline hexamer in the R_6 state there is no observable fast kinetic phase in the terpy reaction and that sequestering and removal of zinc ion from this protein is an extremely slow process provides additional support for the above-stated conclusions about mechanism. If in solution the addition of 0.05–0.1 M phenol converts all of the hexamers to the R_6 form (as found in the crystalline state), then the protein-bound zinc ions are confined to sites within the hexamer that are inaccessible to terpy. Consequently, the likely pathway for the removal of zinc ion by terpy is via the transformation of R_6 to T_6 (perhaps via T_3R_3) followed by the events depicted in eq 1–3. The rate-determining steps (and the overall activation energy) then almost certainly would be dependent upon the dissociation of phenol and the necessary conformational transformations. The observation of a slow, monophasic reaction is consistent with this interpretation.

ACKNOWLEDGMENTS

We thank Dr. Leo B. Snel at the Novo Research Institute for providing the samples of proinsulin and miniproinsulin used in these studies, and we thank Dr. Steven C. Koerber and James Mason for advice and assistance at various stages of the development of the software and hardware for our rapid kinetic systems. We also thank Professor Guy Dodson for providing details of the R_6 structure prior to publication.

Registry No. SCN^-, 302-04-5; miniproinsulin, 119970-48-8.

REFERENCES

Baker, E. N., Blundell, T. L., Cutfield, J. F., Cutfield, S. M., Dodson, E. J., Dodson, G. G., Hodgkin, D. C., Hubbard, R. E., Isaacs, N. W., Reynolds, C. D., Sakabe, K., Sakabe, N., & Vijayan, N. M. (1988) *Philos. Trans. R. Soc. London, B* (in press).

Bentley, G. A., Dodson, E. J., Dodson, G. G., Hodgkin, D. C., Mercola, D. A., & Wollmer, A. (1975) presented at the Spring Meeting of the British Diabetic Association, Sheffield, U.K.

Bentley, G. A., Dodson, E. J., Dodson, G. G., Hodgkin, D. C., & Mercola, D. A. (1976) *Nature 261*, 166–168.

Bentley, G. A., Dodson, G. G., & Lewitova, A. (1978) *J. Mol. Biol. 126*, 871–875.

Blundell, T., Dodson, G. G., Hodgkin, D. C., & Mercola, D. (1972) *Adv. Protein Chem. 26*, 279–402.

Chothia, C., Lesk, A. M., Dodson, G. G., & Hodgkin, D. C. (1983) *Nature 302*, 500–505.

Cutfield, J. F., Cutfield, S. M., Dodson, E. J., Dodson, G. G., Hodgkin, D. C., & Reynolds, C. D. (1981) *Hoppe-Seyler's Z. Physiol. Chem. 362*, 755–761.

De Graaff, R. A. G., Lewit-Bentley, A., & Tolley, S. P. (1981) in *Structural Studies on Molecules of Biological Interest* (Dodson, G., Glusker, J. P., & Sayre, D., Eds.) pp 547–556, Clarendon Press, Oxford, U.K.

Dodson, E. J., Dodson, G. G., Hodgkin, D. C., & Reynolds, C. D. (1979) *Can. J. Biochem. 57*, 469–479.

Dodson, E. J., Dodson, G. G., Hubbard, R. E., & Reynolds, C. D. (1983) *Biopolymers 22*, 281–292.

Dunn, M. F., Bernhard, S. A., Anderson, D., Copeland, A., Morris, R. G., & Rogue, J.-P. (1979) *Biochemistry 18*, 2346–2354.

Dunn, M. F., Pattison, S. E., Storm, M. C., & Quiel, E. (1980) *Biochemistry 19*, 718–725.

Eigen, M. (1967) *Nobel Symp. 5*, 333.

Emdin, S. O., Dodson, G., Cutfield, J. M., & Cutfield, S. M. (1980) *Diabetologia 19*, 174–182.
Frank, B. H., & Veros, A. J. (1968) *Biochem. Biophys. Res. Commun. 32*, 155–160.
Frank, B. H., Veros, A. J., & Pekar, A. H. (1972) *Biochemistry 11*, 4926–4931.
Grant, P. T., Coombs, T. L., & Frank, B. H. (1972) *Biochem. J. 126*, 433–440.
Harding, M. M., Hodgkin, D. C., Kennedy, A. F., O'Connor, A., & Weltzmann, P. D. J. (1966) *J. Mol. Biol. 16*, 212–226.
Havu, N., Lundgren, G., & Falkmer, S. (1977) *Acta Endocrinol. 86*, 570–577.
Howell, S. L. (1974) *Adv. Cytopharmacol. 2*, 319–327.
Howell, S. L., Kostianovsky, M., & Lacy, P. E. (1969) *J. Cell Biol. 42*, 695–705.
Kaarsholm, N. C., & Dunn, M. F. (1987) *Biochemistry 26*, 883–890.
Koshland, D. E., Nemethy, G., & Filmer, D. (1966) *Biochemistry 5*, 365–385.
Markussen, J., Diers, I., Engesgaard, A., Hansen, M. T., Hougaard, P., Langkjaer, L., Norris, K., Ribel, U., Sørensen, A. R., Sørensen, E., & Voigt, H. O. (1987) *Protein Eng. 1*, 215–223.
Monod, J., Wyman, J., & Changeux, J.-P. (1965) *J. Mol. Biol. 12*, 88–118.
Palmieri, R., Lee, R. W.-K., & Dunn, M. F. (1988) *Biochemistry 27*, 3387–3397.
Peking Insulin Structure Research Group (1974) *Sci. Sin. 17*, 779–792.
Permutt, A. (1981) in *The Islets of Langerhans* (Copperstein, S. J., & Watkins, D., Eds.) pp 75–93, Academic Press, New York.
Ramesh, V., & Bradbury, J. H. (1986) *Int. J. Pept. Protein Res. 28*, 146–153.
Reinscheidt, H. Strassburger, W., Glatter, U., Wollmer, A., Dodson, G. G., & Mercola, D. A. (1984) *Eur. J. Biochem. 142*, 7–14.
Sakabe, N., Sakabe, K., & Sasaki, K. (1981) in *Structural Studies on Molecules of Biological Interest* (Dodson, G. G., Glusker, J. P., & Sayre, D., Eds.) pp 509–526, Clarendon Press, Oxford, U.K.
Schlichtkrull, J. (1958) *Insulin Crystals*, pp 1–140, Munsgaard, Copenhagen.
Smith, G. D., Swenson, D. C., Dodson, E. J., Dodson, G. G., & Reynolds, C. D. (1984) *Proc. Natl. Acad. Sci. U.S.A. 81*, 7093–7097.
Snel, L., & Damgaard, U. (1988) *Horm. Metab. Res.* (in press).
Steiner, D. F. (1976) *Diabetes 26*, 322–340.
Steiner, D. R., Hallund, O., Rubenstein, A. H., Cho, S., & Baylis, C. (1968) *Diabetes 17*, 725–736.
Storm, M. C., & Dunn, M. F. (1985) *Biochemistry 24*, 1749–1756.
Williamson, K. L., & Williams, R. J. P. (1979) *Biochemistry 18*, 5966–5972.
Wollmer, A., Rannefeld, B., Johansen, B. R., Hejnaes, K. R., Balschmidt, P., & Hansen, F. B. (1987) *Biol. Chem. Hoppe-Seyler 368*, 903–912.

Selection of a Nucleation-Promoting Element following Chemical Modification of Tubulin†

Tracy M. Sioussat and Kim Boekelheide*
Department of Pathology and Laboratory Medicine, Brown University, Providence, Rhode Island 02912
Received July 12, 1988; Revised Manuscript Received December 7, 1988

ABSTRACT: Following a 16-h incubation with a large excess of 2,5-hexanedione (2,5-HD) while in the assembled state, bovine brain tubulin contained a powerful nucleating component, the presence of which lowered the dissociation rate from 83 s^{-1} for untreated tubulin to 13 s^{-1} for 2,5-HD-treated tubulin. This nucleating component could be selectively concentrated by sequential stringent (conditions of low temperature and low tubulin concentration) cycles of assembly and disassembly. In 2-(*N*-morpholino)ethanesulfonic acid buffer without glycerol, the critical concentration of assembly of untreated tubulin (2.4 mg/mL) was 19 times higher than that of 2,5-HD-treated tubulin subjected to three sequential stringent cycles of assembly and disassembly (0.13 mg/mL). This highly nucleating 2,5-HD-treated tubulin preparation could both copolymerize with untreated tubulin and seed subcritical concentration assembly of untreated tubulin. Experiments to define the assembly-altering component have identified structural alterations to the α-tubulin monomer. While the α-tubulin subunit of native untreated tubulin dimer contained no chymotryptic cleavage sites, the native 2,5-HD-treated α-tubulin subunit was cleaved by chymotrypsin to yield a 37-kDa C-terminal fragment.

Cells are dependent on their cytoskeletons for a variety of their functions. Assembly and disassembly of microtubules into their component tubulin subunits are a necessity for many of these functions. Microtubule assembly and disassembly are required for the development of cell polarity in mouse blastomeres because the microtubules redistribute from the basal to the apical part of the cell (Houliston et al., 1988). During mitosis, the microtubules disassemble from their interphase configurations to assemble into the spindle (Vandre et al., 1984). Chromosome movement toward the spindle poles in metaphase depends upon disassembly of microtubules at their

† This work was supported in part by NIH Grant R01 ES05033 and by the International Life Sciences Institute Research Foundation. A preliminary report was presented at the November 1987 Meeting of the American Society for Cell Biology (Sioussat & Boekelheide, 1987).
* Address correspondence to this author at the Department of Pathology and Laboratory Medicine, Division of Biology and Medicine, Brown University, Box G, Providence, RI 02912.

0006-2960/89/0428-4435$01.50/0